International Journal on Magnetic Particle Imaging
Vol 10, No 1, Suppl 1, Article ID 2403035, 4 Pages

Infinite Science Publishing

Proceedings Article

Design of a hybrid magnetic fluid hyperthermia and magnetic particle spectrometer setup

Ali Hakan Altinay[a,*] · Mustafa Utkur[b,c] · Emine Ulku Saritas[a,d]

[a] Department of Electrical and Electronics Engineering, Bilkent University, Ankara, Turkey
[b] Harvard Medical School, Boston, MA, United States
[c] Boston Children's Hospital, Boston, MA, United States
[d] National Magnetic Resonance Research Center (UMRAM), Bilkent University, Ankara, Turkey
[*] Corresponding author, email: hakan.altinay@ug.bilkent.edu.tr

Abstract

Magnetic particle imaging (MPI) enables cancer imaging via enhanced permeability and retention effect that causes magnetic nanoparticles (MNPs) to accumulate in cancerous tissue, or via determining the change in MNP signal due to increased viscosity in cancerous tissue. MPI can also enable localization of magnetic fluid hyperthermia (MFH) therapy to a targeted region to locally heat up the MNPs and cause the death of cancerous tissue. However, the heating should be kept under control so that the nearby healthy tissue is spared. Hybrid MFH-MPI systems have the potential to enable real-time non-invasive temperature monitoring for hyperthermia therapy via the relaxation response of MNPs. Here, we present the design and simulation results of a hybrid MFH and magnetic particle spectrometer (MPS) setup. This hybrid design is composed of three coaxial coils with gradiometric windings to minimize the mutual inductances among all three coils.

I. Introduction

Magnetic particle imaging (MPI) is a highly promising imaging modality for cancer imaging [1, 2]. MPI can detect cancer by taking advantage of the enhanced permeability and retention effect that accumulates magnetic nanoparticles (MNPs) used as imaging tracers [2], or the local increase in viscosity of cancerous tissue that alters the MNP signal [3]. Furthermore, MPI was shown to enable arbitrary localization of magnetic fluid hyperthermia (MFH) therapy, in which the magnetic nanoparticles (MNPs) heat up and destroy cancerous tissue when exposed to high frequency (e.g., 300-400 kHz) magnetic fields [4]. To prevent damage to the nearby healthy tissue, the local tissue temperature during MFH should ideally be monitored. The temperature-dependent relaxation response of MNPs can enable real-time, non-invasive temperature monitoring with MPI [3]. Therefore, a hybrid MFH-MPI system that can simultaneously image the location of MNPs, perform localized heating, and monitor temperature in real time would be highly beneficial for cancer treatment monitoring.

In this work, we present the design and simulation results of a hybrid MFH and magnetic particle spectrometer (MPS) setup for interleaved heating and temperature monitoring of MNPs. One potential application of this setup is to determine the optimal MFH and MPS operating parameters (e.g., frequency and amplitude) for a given MNP type. This hybrid setup consists of a MFH coil for heating MNPs, and drive and receive coils for

Table 1: Physical design specifications of the coils in the hybrid MFH-MPS setup.

	MFH Coil	Drive Coil	Receive Coil
D_{in} (mm)	58.5	32.0	15.0
D_{out} (mm)	61.5	34.8	18.4
# of Layers	8	8	6
# of Sections	6	6	4
Gradiometer Order	-	First Order	Third Order
Winding directions of sections	[+, +, +, +, +, +]	[+, +,+, -, -, -]	[+, -, +, -]
# of windings per section	[20, 11, 11, 11, 11, 20]	[18, 11, 24, 24, 11, 18]	[40, 46, 46, 40]
Separation between sections (mm)	[14, 14, 14, 14, 14]	[7, 7, 6.5, 7, 7]	[6, 6, 6]
Overall coil lengths (mm)	171	162	156

Table 2: Electrical and magnetic specifications of the coils in the hybrid MFH-MPS setup.

	MFH	Drive	Receive
R_{DC} (Ω)	3.84	2.93	4.83
L (mH)	9.34	4.96	2.27
Sensitivity (mT/A)	3.87	4.89	7.29
95% Homog. Length (cm)	14.87	5.07	1.02

MPS measurements of MNP signal. Because the current passing through one coil can inhibit the other coils by inducing large voltages, the hybrid setup was designed to minimize the mutual inductances among all three coils.

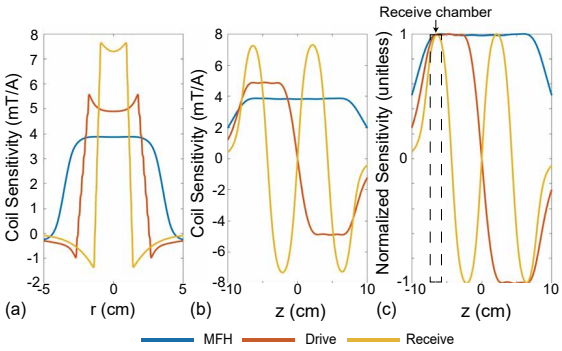

Figure 1: Simulated sensitivity maps of coils in the hybrid setup design, (a) as a function of radial position at z=0 (i.e., at the central plane of the setup), and (b) as a function of z-position at r=0 (i.e., along the axis of the setup). Here, coil sensitivity indicates the magnetic field formed along the z-direction per unit current. (c) Normalized sensitivity maps show that the receive chamber coincides with the peak sensitivity regions of all three coils.

II. Material and methods

In the hybrid MFH-MPS setup, the drive coil and the receive coils were designed as gradiometer coils, whereas the MFH coil was designed as a solenoid. The following sections provide the details of the overall design.

II.I. Mutual Inductance and Gradiometer Coil

The mutual inductance between two coils can be characterized through the coupling coefficient as

$$M = k\sqrt{L_1 L_2}, \tag{1}$$

where M is the mutual inductance, k is the coupling coefficient, and L_1 and L_2 are the self-inductances of the two coils. Here, $0 \leq k < 1$, with $k = 0$ indicating perfectly decoupled coil pairs [5].

Having non-zero mutual inductance can cause the current passing through one coil to induce large voltages on the other coils, preventing the system from operating at the desired performance level. In particular, inducing a large direct feedthrough signal on the receive coil can significantly reduce the quality of the MNP signal. Considering the relatively high MFH frequencies, inducing large voltages on the drive and receive circuitry during MFH can also be problematic. One potential solution for this problem is to geometrically decouple the coils by winding one of the coils in a gradiometric fashion. The gradiometer order of a coil is defined as the number of times the winding direction changes on the coil [6].

II.II. Hybrid MFH-MPS Setup

For the hybrid MFH-MPS setup, 3 coaxial coils were designed: MFH coil, drive coil, and receive coil. The main goals of this design were to minimize mutual inductances and maximize sensitivity and homogeneity, while avoiding system heating. The physical properties of the coils in the hybrid design are given in Table 1. Most notably, the MFH coil was designed as a solenoid without any gradiometric property, whereas the drive coil was designed as a first order gradiometer and the receive coil was designed as a third order gradiometer. To increase the field homogeneity of the MFH coil and drive coil, they were designed to have multiple sections with small separations

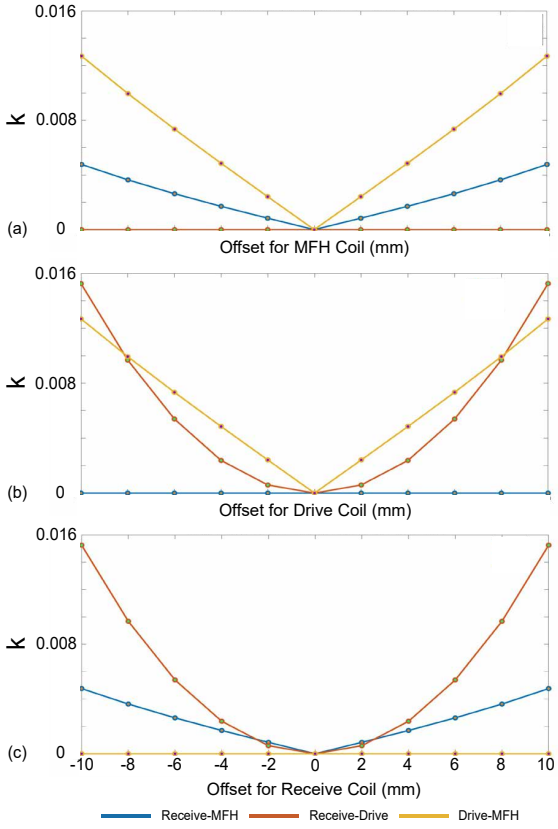

Figure 2: Robustness against positioning offsets for the hybrid setup. Effects of positioning offset for (a) MFH coil, (b) drive coil, and (c) receive coil. Coupling coefficient k among the three coils is calculated via simulations for each offset along the z-direction for a given coil, while keeping other coil positions constant.

in between. A 1.2 mm diameter Litz wire was chosen for the windings of the MFH and drive coils, whereas a 0.8 mm diameter Litz wire was chosen for the receive coil. The individual strand sizes for the Litz wires were chosen to maintain relatively constant resistance values at the targeted frequencies. The targeted frequencies and field amplitudes were 1-25 kHz and 10-15 mT for the drive coil, and 200-400 kHz and 5-10 mT for the MFH coil. The number of windings on each section, the winding directions, and the separations between sections were adjusted to make the mutual inductance values zero for all three coils, as well as to ensure that the homogeneous regions of the coils align well. The number of winding layers was determined to ensure that the current density for the MFH coil and drive coil remained below 5 A/mm^2 at the targeted field amplitudes to avoid resistive heating. For the MFH coil and drive coil, the number of layers was determined based on this rule-of-thumb limit.

Magnetic field simulations and mutual inductance computations were performed using a custom script in MATLAB. First, the magnetic field due to a unit current passing through a given coil was computed using the Biot-Savart law. Then, the mutual inductance between that coil and a secondary coil was calculated by adding the total fluxes through each turn of the secondary coil [5].

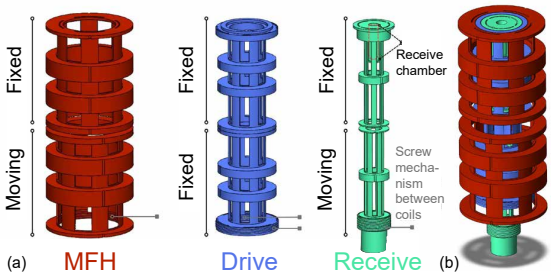

Figure 3: 3D SolidWorks design of (a) MFH, drive, and receive coils and (b) the overall hybrid MFH-MPS setup. The drive coil is fixed, whereas the lower halves of MFH and receive coils are movable to minimize mutual inductances.

III. Results and discussion

Table 2 shows the calculated electrical and magnetic specifications of the coils, whereas Fig. 1 displays the sensitivity maps of the coils. The sensitivity profiles reflect the gradiometric properties of the drive and receive coils. The high sensitivity for the receive coil and the extended homogeneity area for the MFH and drive coils indicate that the design goals are met. The sensitivity maps in Fig. 1 show that the peak sensitivity regions of all three coils align well, forming a suitable receive chamber region for sample placement within the setup.

Next, Fig. 2 displays robustness analysis for the mutual inductances of the three coils. In this analysis, the position of one of the coils was offset along the z-direction, and the coupling coefficients among the three coils were recomputed for each offset value. In the case of zero offsets, the three coils have zero mutual inductances (i.e., zero coupling coefficients indicating that the coils are completely decoupled). Even at an offset of 1 cm, the coupling coefficients remain below 0.016, maintaining a relatively good decoupling level of more than 35 dB decoupling. These results demonstrate the robustness of the designed hybrid system against positioning errors.

Finally, the 3D design of the hybrid setup is shown in Fig. 3. The drive coil was fixed completely, as well as the upper halves of the MFH and receive coils. This way, field homogeneity and sensitivity over the receive chamber will not change with coil adjustments. The lower halves of the MFH and receive coils were movable via screw mechanisms. These movable parts were designed to tune the position of the coils to compensate for non-idealities during implementation, enabling the minimization of the mutual inductances among the three coils. To accommodate for potential air cooling of the coils, 2 mm gaps were left in between the coils along the diameter

direction. The next step will be to implement and test the MFH and MPS capabilities of this hybrid system, followed by interleaved heating and temperature monitoring of MNPs.

IV. Conclusions

In this work, we presented the design of a hybrid MFH-MPS setup, where all three coils were designed to have zero mutual inductances. This system maintains high sensitivity and homogeneity within the receive chamber and is robust against positioning errors.

Acknowledgments

This work was supported by the Scientific and Technological Research Council of Turkey (TUBITAK 122E162).

Author's statement

Conflict of interest: Authors state no conflict of interest.

References

[1] E. U. Saritas, P. Goodwill, L. Croft, J. Konkle, K. Lu, B. Zheng, and S. Conolly. Magnetic particle imaging (mpi) for nmr and mri researchers. *Journal of Magnetic Resonance*, 229:116–126, 2013, doi:10.1016/j.jmr.2012.11.029.

[2] E. Y. Yu, M. Bishop, B. Zheng, R. M. Ferguson, A. P. Khandhar, S. J. Kemp, K. M. Krishnan, P. W. Goodwill, and S. M. Conolly. Magnetic particle imaging: A novel in vivo imaging platform for cancer detection. *Nano Letters*, 17(3):1648–1654, 2017, PMID: 28206771. doi:10.1021/acs.nanolett.6b04865.

[3] M. Utkur and E. U. Saritas. Simultaneous temperature and viscosity estimation capability via magnetic nanoparticle relaxation. *Medical Physics*, 49(4):2590–2601, 2022, doi:10.1002/mp.15509.

[4] Z. W. Tay, P. Chandrasekharan, A. Chiu-Lam, D. Hensley, R. Dhavalikar, X. Zhou, E. Yu, P. Goodwill, B. Zheng, C. Rinaldi, and S. Conolly. Magnetic particle imaging-guided heating in vivo using gradient fields for arbitrary localization of magnetic hyperthermia therapy. *ACS Nano*, 12(4):3699–3713, 2018, doi:10.1021/acsnano.8b00893.

[5] I. Mayergoyz and W. Lawson, Chapter 10 - magnetically coupled circuits and two-port elements, in *Basic Electric Circuit Theory*, I. Mayergoyz and W. Lawson, Eds., San Diego: Academic Press, 1997, 381–430, ISBN: 978-0-08-057228-4. doi:https://doi.org/10.1016/B978-0-08-057228-4.50014-8.

[6] S. Tumański. Induction coil sensors—a review. *Measurement Science and Technology*, 18(3):R31–R46, 2007, doi:10.1088/0957-0233/18/3/r01.

